HYDROLOGICAL PROCESSES
Hydrol. Process. **18**, 2103–2116 (2004)
Published online in Wiley InterScience (www.interscience.wiley.com). DOI: 10.1002/hyp.5559

Seasonal inundation patterns in two large savanna floodplains of South America: the Llanos de Moxos (Bolivia) and the Llanos del Orinoco (Venezuela and Colombia)

Stephen K. Hamilton,[1]* Suzanne J. Sippel[1,2] and John M. Melack[2]

[1] *W.K. Kellogg Biological Station and Department of Zoology, Michigan State University, 3700 E. Gull Lake Drive, Hickory Corners, Michigan 49060-9516, USA*

[2] *Institute for Computational Earth System Science and Bren School for Environmental Science and Management, University of California, Santa Barbara, California 93106-3060, USA*

Abstract:

Inundation patterns in two of the largest savanna floodplains of South America were studied by analysis of the 37-GHz polarization difference observed by the Scanning Multichannel Microwave Radiometer (Nimbus-7 satellite). Flooded area was estimated at monthly intervals for January 1979 through to August 1987 using mixing models that account for the major landscape units with distinctive microwave emission characteristics. Results are presented separately for five subregions in each of the two floodplain regions to show the spatial as well as temporal variability in inundation patterns. The total area inundated during the 9 years varied between 2069 and 78 460 km^2 in the Llanos de Moxos (also spelled as Mojos; median area, 23 383 km^2) and 1278 and 105 454 km^2 in the Llanos del Orinoco (median, 25 374 km^2), not including the open-water area of permanent lakes and river channels. The correlation between flooded area and river stage was used to extend the inundation records over a 30-year period in the Moxos (1967–97) and a 58-year period (1927–85) in the Orinoco. Interannual variability in inundation is greater in the Moxos than the Orinoco. Comparison of these data, however, with a previously published analysis of the Pantanal wetland shows that inundation patterns in these two floodplain regions are not as variable across years as they are in the Pantanal. Copyright © 2004 John Wiley & Sons, Ltd.

KEY WORDS remote sensing; floodplain; hydrology; passive microwave emission; SMMR; Orinoco River; Madeira River; Llanos de Mojos; Llanos de Moxos

INTRODUCTION

Seasonal inundation in the floodplains along large rivers in South America exerts fundamental control on the biogeochemistry and ecology of these ecosystems (Junk *et al*., 1989; Lewis *et al*., 2000). Knowledge of the spatial and temporal variability of inundation provides a foundation for basic biogeochemical and ecological studies, as well as for the conservation and management of natural resources (Junk, 1997) and for analyses of the environmental impact of river channel modifications such as dredging or impoundment (Hamilton, 1999). Hydrological and biogeochemical models of riverine systems require information on inundation patterns to account for exchanges of water between rivers and their floodplains, as residence of water in floodplains can result in large evaporative losses and substantial alterations in riverine fluxes of dissolved and particulate materials (Lewis and Saunders, 1989; Richey *et al*., 1989; Mertes *et al*., 1996; Hamilton *et al*., 1997). Data on the total area and duration of flooding are also required to estimate methane emissions from floodplains,

* Correspondence to: Stephen K. Hamilton, Kellogg Biological Station and Department of Zoology, Michigan State University, 3700 E. Gull Lake Drive, Hickory Corners, MI 49060-9516, USA. E-mail: Hamilton@kbs.msu.edu

Received 6 January 2003
Accepted 6 October 2003

which occur largely during the inundation phase, and South American floodplains are a significant source of atmospheric methane on a global scale (Bartlett and Harriss, 1993; Smith *et al*., 2000).

Inundation patterns in the major floodplains of South America have until recently been poorly known because of the vast size and remoteness of these areas and the difficulty of using optical remote sensing technologies such as Landsat in humid regions, where cloud cover limits the ability to acquire multiple images over time. Passive microwave remote sensing from satellites can reveal the presence of surface water despite cloud cover. We have developed methods to determine flooded area from the 37-GHz polarization difference observed by the Scanning Multichannel Microwave Radiometer (SMMR), operated on board the Nimbus-7 satellite from January 1979 through to August 1987. In previous publications we have described our methods in detail and presented results for the fringing floodplains of the central Amazon River system and four of its major tributaries (Sippel *et al*., 1994, 1998), and for the Pantanal wetland in Brazil (Hamilton *et al*., 1996; Hamilton, 1999). In each floodplain region, we estimated inundation area separately for subregions using mixing models that account for the major landscape units with distinctive microwave emission characteristics. Hamilton *et al*. (2002) synthesized results from the above studies as well as the present one to compare the regional inundation patterns among the major floodplains of South America.

In this study, we determined inundation patterns from the SMMR observations in two of the major savanna floodplains of South America: (i) the Llanos de Moxos in Bolivia; and (ii) the Llanos del Orinoco in Venezuela and Colombia. We present data on the spatial and temporal patterns of inundation in these two regions, and we compare inundation patterns in these regions with our previously published observations on the central Amazon floodplain and the Pantanal wetland. Historical records of river stage are combined with empirical relationships between river stage and flooded area to extend the inundation record over longer periods and examine interannual variability in inundation in these floodplain regions.

The locations of the two floodplain regions analysed in this study as well as the previously studied Pantanal wetland are depicted in Figure 1. Each of these floodplain regions is associated with a major river system, although inundation is not necessarily driven entirely by overbank discharge from the parent rivers. These three floodplain regions comprise much of the total savanna floodplain area in the continent, but significant savanna floodplains are also found in the Amazon River system, including the Roraima savannas of the Branco River watershed and Bananal island on the Araguaia River, and down-river of the Pantanal in the Paraguay and Paraná river watersheds (Junk, 1993).

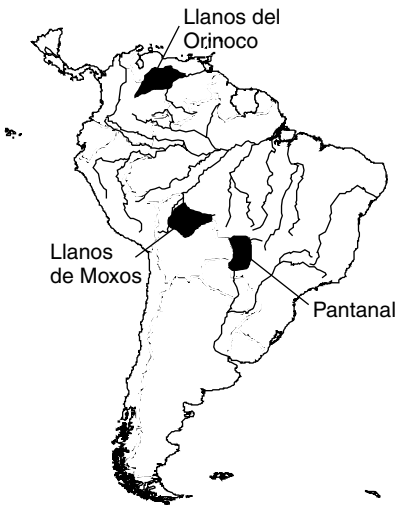

Figure 1. Map of South America showing the location of the floodplain regions considered in this study as well as the Pantanal wetland, another large savanna floodplain

LLANOS DE MOXOS (BOLIVIA)

The Llanos de Moxos (also spelled as Mojos) is a savanna region of approximately 150 000 km^2 located in the upper Madeira River watershed in northeastern Bolivia, between the Beni, Mamoré and Guaporé (or Iténez) rivers (Figure 2). In this region, the natural vegetation tends to be evergreen forest in areas that are not subject to seasonal inundation, and inundation tends to maintain grassland or savanna vegetation (Langstroth, 1996). Deforestation and burning for pasture may have resulted in extension of savanna into previously forested areas. The Beni and Mamoré rivers drain montane watersheds of the Andes and carry mean annual discharges of 9000 and 8400 m^3/s, respectively, and the Guaporé River drains lower elevations to the east in Bolivia and Brazil and carries a mean annual discharge of 2125 m^3/s (Guyot and Wasson, 1994). River discharge is strongly seasonal and results in large fluctuations in water level, reaching 11 m in the Mamoré River channel, although the river channels are incised into the plains and the depth of inundation in most of the savanna areas remains <1 m (Hanagarth, 1993). Mean annual precipitation varies from 1300 to 2000 mm across the region, occurring mostly between September and May (Denevan, 1966; Hanagarth, 1993). The sediments comprising the Moxos floodplains are largely alluvial deposits from the late Pleistocene and Holocene that have filled a pericratonic basin (Campbell *et al*., 1985); granitic outcrops of the Brazilian shield along the rivers to the north constrain the channels and contribute to a backwater effect at high water. Fine-textured soils with poor infiltration are common on the floodplains (Haase, 1992; Langstroth, 1996). The floodplain has been sculpted by numerous former river channels that carry overbank river flow or local runoff during the wet season (Hanagarth, 1993). The most important floodplain lakes include several large basins with rectangular shapes that reflect the underlying lineaments of the basement rock (Plafker, 1964), as well as numerous smaller lakes formed by migrating river channels, particularly along the Mamoré River (Hanagarth, 1993).

The Beni subregion contains water courses that drain mainly toward the Mamoré River to the east, probably reflecting former courses of the Beni River (Hanagarth, 1993). Vegetation to the east of the Beni River is mostly savanna but also includes some marshes of the sedge *Cyperus giganteus*. West of the Beni River there is more evergreen forest that is subject to the variable degrees of inundation (Haase and Beck, 1989; Beck and Moraes, 1997). The Mamoré subregions encompass the fringing floodplain of the Mamoré River, which contains gallery forest and abundant floodplain lakes, as well as outlying savannas that appear to be subject to backwater effects of the Mamoré River. Open palm stands of various species are abundant in the savannas to the east of the Mamoré River, including much of the Baures subregion (Beck and Moraes, 1997). The Mamoré subregions have been divided arbitrarily into southern (up-river) and northern (down-river) halves. The Mamoré North subregion was extended to the west to encompass a particularly large lake and associated

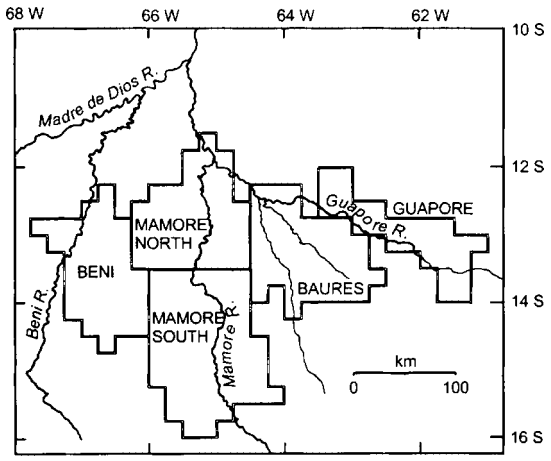

Figure 2. Subregions in the Llanos de Moxos (Bolivia)

marshes called Rogoaguado. The Baures subregion covers the remaining savanna floodplain to the east of the Mamoré subregions and to the south of the Guaporé (Iténez) River. The Guaporé subregion, located primarily to the north of the Guaporé River, is outside the area traditionally known as the Moxos but was included here because of its proximity and significant extent.

LLANOS DEL ORINOCO (VENEZUELA AND COLOMBIA)

The Llanos del Orinoco is a region of alluvial plains occupying approximately 150 000 km^2 between the Orinoco River and the Andean foothills (Figure 3). In contrast to the Llanos de Moxos region, the climate here tends to support savanna vegetation regardless of whether seasonal inundation occurs (Sarmiento, 1983). Extensive areas of savanna also occur all along the north side of the Orinoco River to its mouth, and these areas are often considered together with the savanna floodplains as a single physiographic unit denominated as the Llanos del Orinoco (e.g. Tamayo, 1961; Sarmiento, 1983). In this study, however, we define the Llanos del Orinoco as the lower lying savanna areas that are subject to seasonal inundation. We exclude the more upland savannas to the east because most of that region is not contiguous floodplain and bears a closer resemblance to the Cerrado savannas of Brazil (San José and Montes, 1989; Montes and San José, 1995). The floodplains of this region are drained by two major tributaries of the Orinoco River, both of which originate in the Andes: the Apure River (mean annual discharge, 2300 m^3/s) and the Meta River (5600 m^3/s) (Lewis *et al*., 1995). River channels within the Llanos del Orinoco tend to be braided, and much water flows outside the main channels during inundation (Pérez Hernández and Luís López, 1998). Mean annual precipitation in the region is about 1500 mm, occurring mostly between June and August, with higher precipitation in the upland watersheds of the Andes.

The Casanare subregion, named for the river that drains its floodplains and flows into the Meta River, lies in Colombian territory. Little scientific information is available on this area, but examination of satellite images as well as a map in Sarmiento (1983) shows that it is largely savanna. The floodplains between the Apure and Meta rivers include the Arauca and Capanaparo subregions. Ramia's (1967) vegetation map shows grasslands composed largely of *Paspalum fasciculatum* in the Arauca area and of *Trachypogon* spp. in the Capanaparo area. The Guanare subregion encompasses the savanna floodplains to the north of the Apure River, which intergrade into more upland savanna environments to the north. The Apure Delta subregion covers the internal delta at the confluence of the Apure with the Orinoco River, and extends across the Orinoco River to cover savanna floodplains on the other side of the fringing floodplain of the Orinoco. The fringing floodplain of the Orinoco in this area is forested and contains numerous floodplain lakes (Hamilton and Lewis, 1990), but it occurs as a narrow strip that could not be analysed separately in this study, so it was included in the adjacent

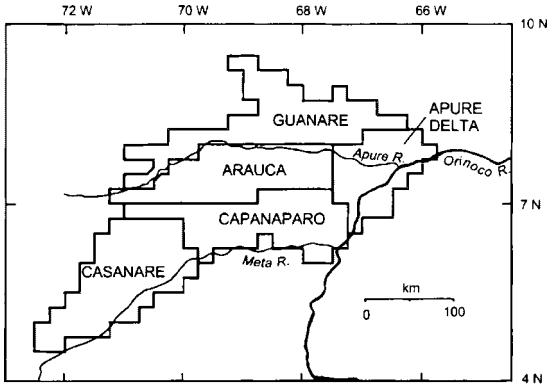

Figure 3. Subregions in the Llanos del Orinoco (Venezuela and Colombia)

Apure Delta subregion. Inundation in the Apure Delta subregion is subject to backwater effects of the Orinoco (Meade *et al*., 1983; Herrera and Rondón, 1985), potentially producing a rather different inundation regime compared with the rest of the region.

METHODS

SMMR data characteristics

The SMMR instrument measured the natural emission of microwave energy from Earth's surface and atmosphere. Measurements are expressed as brightness temperatures (in Kelvins), and are available at several frequencies and at both vertical and horizontal polarizations (Fu *et al*., 1988). The difference between vertically and horizontally polarized brightness temperatures observed by satellite at the 37 GHz frequency (hereafter referred to as ΔT_{obs}) provides a sensitive indicator of the presence of surface water, particularly where water occurs against a background of vegetated land surfaces (Choudhury, 1991). Choudhury (1989) reviewed the theoretical basis for interpretation of 37 GHz emission. The spatial resolution of the SMMR sensor is approximately 27 km at 37 GHz and the processed global data set is gridded into cells of 0·25° latitude by longitude.

Satellite observations of 37 GHz emission are available for December 1978 to August 1987 from the SMMR instrument operated on board the Nimbus-7 satellite (Fu *et al*., 1988; Gloersen *et al*., 1992). In this study, we use the monthly SMMR observations originally described by Choudhury (1991). Global SMMR observations are available for approximately 6-day intervals, and are compiled separately for day and night (local Equator crossings at noon and midnight). After calculation of ΔT_{obs} for each grid cell from the daytime brightness temperatures, the observations were ranked within each month and the second lowest value (usually out of four) was selected, thereby yielding one ΔT_{obs} value per month (Choudhury, 1989). This screening served to eliminate outlying values that might have resulted from atmospheric scattering by heavy rainfall, or from temporary pooling of water on the land surface after heavy rainfalls.

General approach

Our general approach to determine inundation area from the SMMR ΔT_{obs} has been described in detail in Hamilton *et al*. (1996) and Sippel *et al*. (1998) and will only be briefly summarized here, with additional site-specific details provided for the new data we present. We calculated the fractional inundation area within an aggregate of SMMR grid cells using linear mixing models that account for the microwave emission of the major landscape units, or end members, within the subregion (Sippel *et al*., 1994). The end members in these models are flooded land (ΔT_f), non-flooded upland or floodplain (ΔT_{nf}), and open water of permanent lakes and river channels (ΔT_w). The ΔT_f values for flooded land were determined empirically for each subregion because they are expected to vary, primarily as a function of the density and structure of vegetation canopies overlying the water. The ΔT_{nf} values for non-flooded land were also determined empirically by examination of observations made over floodplain areas in the dryest periods, as well as examination of the seasonality of ΔT_{obs} measured over upland areas with comparable vegetation cover. The ΔT_w value for open water cannot be determined empirically in these floodplain regions; we used a theoretical value of 60 K (Choudhury, 1989) that is supported by empirical observation from other regions (Sippel *et al*., 1994). There is little open water in the Moxos and Orinoco floodplains, however, so the accuracy of this end member is not critical to our results.

The approximate boundaries of the Moxos and Orinoco floodplains were delineated using maps, remote sensing and scientific publications, and by examination of the SMMR data for evidence of inundation. The SMMR observations were overlain on the river layer of the digital chart of the world using a geographical information system. For each region we distinguished five subregions that correspond approximately with hydrogeomorphological provinces, although the subregion boundaries are dictated by the coarse resolution of

the SMMR data. Subregion boundaries were chosen to encompass the floodplain subject to inundation and therefore include some upland area along the outer edges. The boundaries were altered in some cases to avoid crossing or bordering major open-water features such as the largest floodplain lakes (Moxos) or river channels (Orinoco mainstem).

After delineating the subregions, the next step was to locate test cells in each subregion, which are SMMR grid cells that are entirely subject to inundation in most years and can be used to determine the ΔT_f value for the subregion under conditions of complete inundation (Sippel *et al*., 1994). All of the sources of information available to us, which are described below for each region, were considered in the selection of test cells. We also measured open-water area of lakes and river channels within each subregion. The fractional inundation area within each subregion was calculated for each monthly ΔT_{obs} observation, and inundation areas of the subregions were summed to yield the total inundation area for the region. Inundation area includes the permanent open-water area of river channels and floodplain lakes.

Concurrent data on river levels (stage) from sites with long records were examined to produce a predictive relationship between river stage and flooded area for each region. We also checked for correlations between monthly rainfall and flooded area, but in both the Moxos and the Orinoco floodplains the river stage yielded a superior correlation. Mean monthly stage was computed, and cross-correlation analyses between the stage and flooded area time-series were performed to check for time lags of 1 month or more. Polynomial regression analysis yielded a predictive equation to extend the inundation record over the period of river stage observations (Sippel *et al*., 1998).

Llanos de Moxos

The five subregions for the Llanos de Moxos are depicted in Figure 2. The areas subject to seasonal inundation were determined from the observed variability in ΔT_{obs}; all contiguous grid cells displaying a standard deviation $>1{\cdot}5$ K over the entire 9 years of observations were included. The total area potentially subject to seasonal flooding in the Moxos corresponds approximately with the distribution of contiguous savanna in the region, because the surrounding upland areas are largely covered by evergreen forest (Langstroth, 1996; Beck and Moraes, 1997). Hydrological flow paths were ascertained from the 1:500 000 scale Tactical Pilot Charts, nine of the 1:250 000 scale maps for the region produced by the Bolivian Government, and information in Hanagarth (1993). There are isolated areas of oligotrophic savanna to the west of the Beni subregion that probably experience some flooding (Beck and Moraes, 1997), but not enough to significantly elevate the SMMR polarization difference at 37 GHz.

In addition to maps, we examined the following resources to delineate subregions and choose test cells in the Moxos region: (i) Landsat-TM images from the NASA Landsat Pathfinder Humid Tropical Forest Inventory Project and also images and other information in Hanagarth (1993); (ii) a map of the distribution of vegetation published in Beck and Moraes (1997); and (iii) mosaic images made from the satellite-borne JERS radar for October–November 1995 and May–June 1996. The area of permanent open water was measured from the Tactical Pilot Charts after verifying that the lake shapes and sizes on these charts corresponded well with the Landsat and JERS images. We used a ΔT_{nf} of $4{\cdot}2$ K for the Moxos, which is the mean of a large number (1664) of ΔT_{obs} measurements over the Gran Chaco savannas of south-eastern Bolivia and northern Paraguay; we used the Chaco region because nearly all of the extensive savanna in the Moxos region is subject to at least some inundation and surrounding uplands are densely forested. We located three to five test cells in each subregion for the determination of ΔT_f.

Stage data for rivers within the Moxos floodplains were not available for extended periods; the best record that we could obtain was for Porto Velho on the Madeira River, down-river from the Llanos de Moxos (Figure 2). The Porto Velho stage record, which extends from 1967 to 1997, was obtained from the Brazilian Government.

Llanos del Orinoco

The five subregions for the Llanos del Orinoco are depicted in Figure 3. As with the Moxos, we delineated the areas subject to inundation using the standard deviation of the SMMR observations, except that for the Orinoco we chose a threshold standard deviation of 1 K because that corresponded better with our other sources of information. To delineate subregions and choose test cells in the Orinoco region, we used the following resources: (i) 1:250 000 scale topographic maps produced by the Venezuelan Government; (iii) 1:500 000 scale Tactical Pilot Charts; (iii) satellite images of the normalized vegetation difference index (derived from the NOAA Advanced Very High Resolution Radiometer) for representative wet- and dry-season dates, which were produced by Milton Smith of the University of Washington; (iv) a vegetation map in Ramia (1967) and a description of the vegetation in the region in Sarmiento (1983). We also had some field experience in the region, and we examined aerial photographs we had taken when we flew across the Llanos during the dry season in December 1985. We used measurements of the open-water area in the region reported by Hamilton and Lewis (1990), who had made planimetric measurements of permanent lakes and river channels marked on the 1:100 000 scale topographic maps produced by the Venezuelan Government.

The subregion boundaries in the Llanos del Orinoco primarily reflect hydrological flow paths and geomorphology. Herrera and Rondón (1985) note that the backwater effect of the Orinoco River can extend up-river along the Apure River to the town of San Fernando de Apure, and stage data in Saunders and Lewis (1988) show that the river level there exceeds 40 m above sea level at high water. Therefore we chose the 40-m elevation contour to define the boundaries of the Apure River subregion, and selected grid cells to encompass that contour. We used a detailed elevation map from an unpublished Venezuelan Government study on the feasibility of an Orinoco dam ('El Infierno') to locate the 40-m contour. The other subregions were defined primarily on the basis of channel flow patterns.

In our previous work in the central Amazon basin and in the Pantanal region, we observed that upland areas covered by savanna or forest vegetation tend to have a mean ΔT_{nf} of ca. $4 \cdot 2 \pm 1 \cdot 0$ K(mean $\pm$ SD) throughout the year (Sippel *et al*., 1994; Hamilton *et al*., 1996; also see above), which is expected as a result of attenuation of the microwave emission by vegetation canopies that completely cover the soil (Choudhury 1989). Justice *et al*. (1989), however, analysed the seasonal variability of ΔT_{obs} in savanna regions throughout the world and found that areas where soils are exposed among the vegetation have significantly elevated ΔT_{obs} values because the attenuating effect of the vegetation on emission from underlying soils is reduced. We observed significant seasonal variation in the ΔT_{obs} in upland savannas to the north-east of the Guanare subregion, where exposed sand and lateritic soil crusts are common and herbaceous biomass is reduced during the dry season (Sarmiento, 1983). In those upland savannas, the ΔT_{obs} was lowest at the end of the wet season ($5 \cdot 5-6 \cdot 5$ K) and increased to its maximum of *c*. 9 K by the end of the dry season, suggesting that soil moisture status is not the cause of the seasonal increase. We suspect a similar seasonal increase during the dry season in some floodplain savannas within the Llanos del Orinoco. The ΔT_{obs} did not fall to *c*. $4 \cdot 2$ K during the dry seasons of the 9-year time-series, even though all the subregions except the Apure Delta are expected to be virtually dry by the end of the dry season in most years, as we observed in our dry-season overflight. We observed bare soil and sand areas during our overflight of the region, and exposed sand is especially common in the eastern part of the Capanaparo subregion (Sarmiento, 1983; Nordin and Pérez Hernández, 1989). Therefore for each subregion we determined ΔT_{nf} empirically from the mean minimum ΔT_{obs} of the four lowest years, correcting for the open-water fraction using a two-end-member mixing model (Sippel *et al*., 1994). This could not be done in the Apure Delta subregion, however, because it does not dry entirely (Herrera and Rondón, 1985). As there is denser vegetation and little exposed soil in that subregion, we used the ΔT_{nf} of $4 \cdot 2$ K that would be expected for a densely vegetated land surface.

As in the case of the Moxos, stage data for rivers within the Llanos del Orinoco were available only for limited periods, although we were unable to locate a longer record that evidently exists for the Apure River at San Fernando de Apure. We did, however, have access to a nearly complete stage of record for 1927 to 1985

from the Ciudad Bolívar station, located down-river on the Orinoco mainstem, so this was used for extension of the inundation record.

RESULTS AND DISCUSSION

Table I shows the measurements of fractional open-water area and the empirically determined values of ΔT_f and ΔT_{nf}. Open-water area in the Llanos de Moxos covers 4780 km^2, of which 77% occurs as lakes and the remainder as river channels. Open-water area in the Llanos del Orinoco occurs largely as river channels, including some of the Orinoco River mainstem, and comprises only 2080 km^2. In the case of the Orinoco River, a substantial fraction (up to 40%) of the river channel becomes exposed as sand bars at low water (Nordin and Pérez Hernández, 1989). We did not account for the microwave emission of these temporarily exposed sand bars, which would only have an impact on our inundation estimates at extreme low water. The resultant error, however, may not be large because relatively flat expanses of sand are expected to yield a ΔT that resembles that of open water (Choudhury, 1989). The ΔT_f values in Table I resemble values we previously documented for subregions in the Pantanal wetland of Brazil that have savanna vegetation and shallow inundation depths (Hamilton *et al*., 1996).

Inundation patterns for subregions of the Llanos de Moxos are presented in Figure 4. Most years showed a unimodal rise and fall in flooded area, although multiple flood peaks occurred occasionally, especially in the Beni and Mamoré South subregions. Although most of the area subject to inundation became dry during the dry season, significant flooded area did persist during the dry season in most years. There is notable variability among the subregions in both the degree of flooding and in the degree of desiccation in a particular year, reflecting the variable sources of floodwaters, which include several distinct upland watersheds as well as local precipitation (Hanagarth, 1993). Denevan (1966) noted that the largest floods result not from local precipitation on the floodplains but from overbank flow of river discharge originating as runoff from the eastern Andes, where precipitation is generally higher. The Beni and Mamoré rivers each drain substantial areas of montane watershed.

Inundation patterns for subregions of the Llanos del Orinoco are presented in Figure 5. The unimodal inundation pulse is more regular than in the Llanos de Moxos. The drainage of the floodplains during the dry season is more complete and consistent among years compared with the Moxos, except in the Apure Delta subregion, which retains significant flooded area during the dry season. As in the Moxos, the interannual

Table I. Characteristics of the grid-cell aggregates for each floodplain subregion. The table shows the number of grid cells that were aggregated to encompass the subregion, the fractional area of open water (f_w, which includes river channels and lakes), and the empirically determined mean values of ΔT_{nf} and ΔT_f (in Kelvins; see text for explanation). The area of a grid cell is *c.* 765 km^2

Floodplain		Grid cells	f_w	ΔT_{nf}	ΔT_f	Number of test cells for ΔT_f
Region	Subregion					
Llanos de Moxos	Beni	38	0·024	4·2	26·3	4
	Mamoré North	40	0·069	4·2	32·4	4
	Mamoré South	58	0·031	4·2	28·6	5
	Baures	41	0·015	4·2	26·2	4
	Guaporé	27	0·006	4·2	21·3	3
Llanos del Orinoco	Guanare	51	0·004	5·1	24·9	3
	Arauca	42	0·009	4·9	25·2	21
	Capanaparo	44	0·009	6·2	24·5	8
	Casanare	52	0·009	4·4	23·3	7
	Apure Delta	30	0·042	4·2	29·3	9

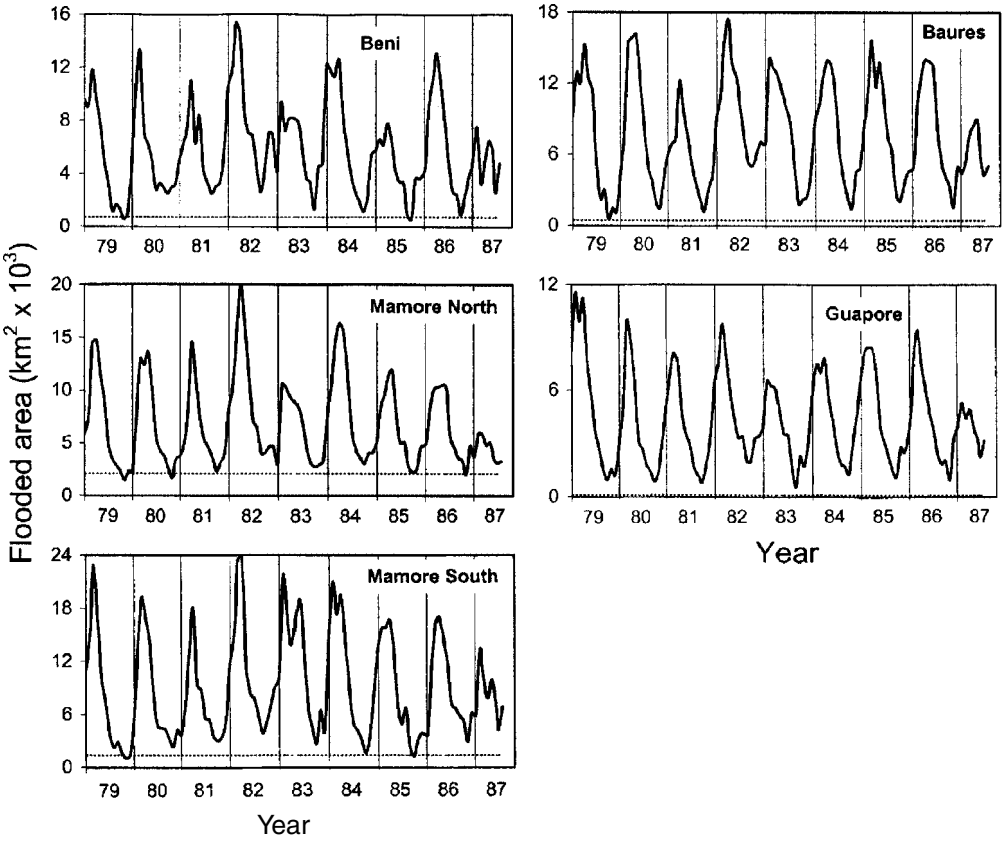

Figure 4. Monthly estimates of flooded area (inundated floodplain plus open water of rivers and lakes) in the five subregions of the Llanos de Moxos. The dashed lines show the area of open water, which is assumed to change little throughout the year

variability in the total flooded area is substantial and variable among the five subregions. The variation in flooding can be explained not only by spatial variation in rainfall on the floodplains but also by the distinct upland watersheds that contribute to discharge of the major rivers crossing the floodplains.

Time-series of the total flooded area in each of the regions show that the total extent of inundation in these floodplains varies among years by about a factor of two (Figure 6). The maximum area subject to simultaneous inundation in the Llanos de Moxos during the SMMR observations was 78 460 km^2 (not including open-water area), which is considerably smaller than the 150 000 km^2 estimated by Junk (1993) based on a review of previously published estimates, but closer to the 100 000 km^2 estimated for years of normal precipitation by Hanagarth (1993). The Llanos del Orinoco showed a larger maximum seasonally inundated area of 105 454 km^2, which exceeds the 80 000 km^2 estimate given by Junk (1993) as well as the 'over 70 000 km^2' reported by Welcomme (1985). Thus the SMMR observations indicate that there is more land subject to seasonal inundation in the Llanos del Orinoco, although the median values of inundation area in the two floodplain regions were similar (23 383 and 25 374 km^2 for the Moxos and Orinoco, respectively). For comparison, during the same period the Pantanal wetland showed a maximum seasonally flooded area of 109 590 km^2 and a median of 54 330 km^2 (Hamilton *et al.*, 1996).

The mean seasonal cycles in flooded area over the SMMR observation period are depicted in Figure 7, together with the ranges observed during each month. The difference in timing of inundation reflects the locations of these regions relative to the Equator and the intertropical convergence zone (Hastenrath, 1990). The dry seasons are relatively predictable in both regions and especially so in the Llanos del Orinoco,

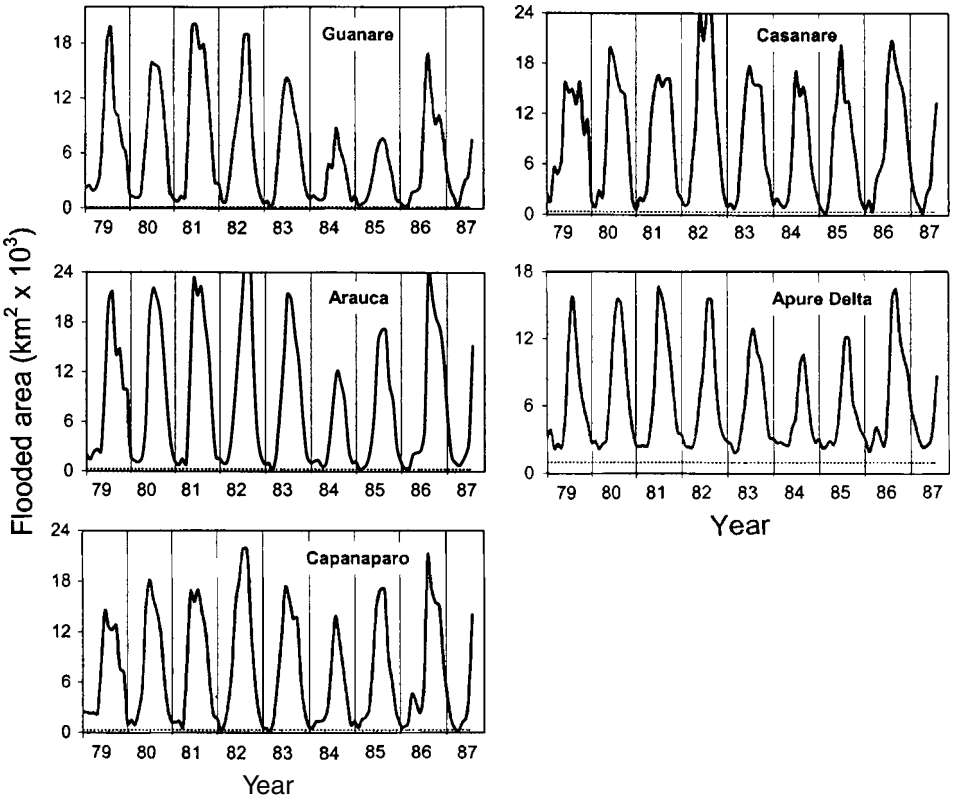

Figure 5. Monthly estimates of flooded area (inundated floodplain plus open water of rivers and lakes) in the five subregions of the Llanos del Orinoco. The dashed lines show the area of open water, which is assumed to change little throughout the year

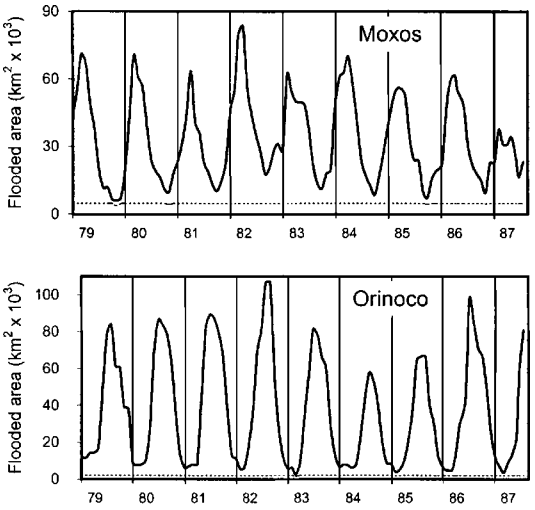

Figure 6. Monthly estimates of total flooded area (inundated floodplain plus open water of rivers and lakes) derived from SMMR satellite observations of passive microwave emission. The dashed lines show the area of open water that changes little throughout the year

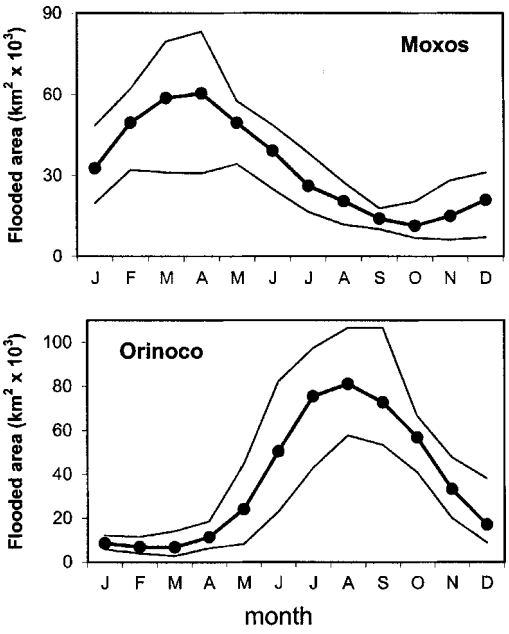

Figure 7. Mean seasonal cycles in flooded area over the period of satellite observations. The lines show the minima and maxima observed in each month over the 9 years

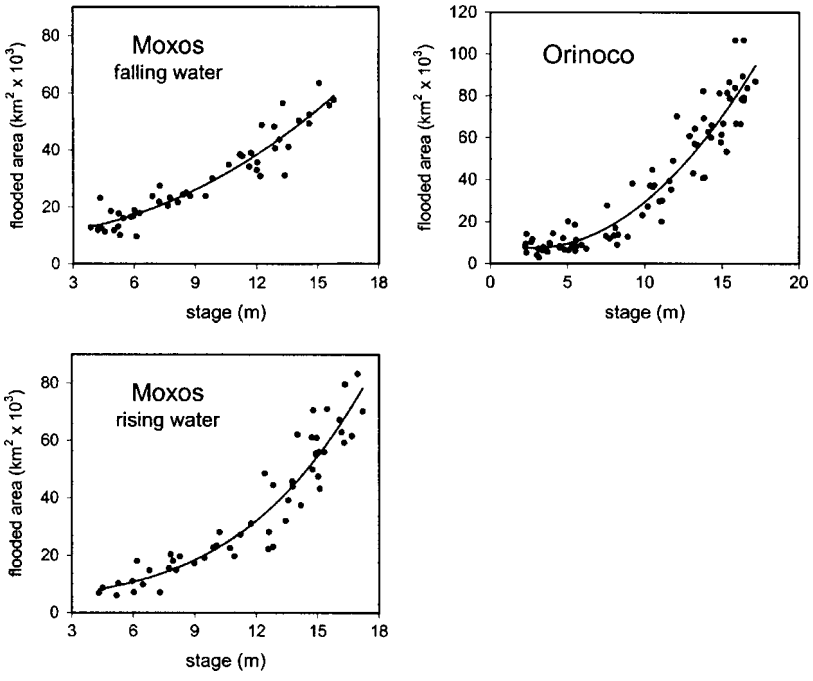

Figure 8. Relationships between monthly river stage and total flooded area for the Llanos de Moxos and Llanos del Orinoco. Open-water area is included in the total flooded area. River stage stations are Porto Velho on the Madeira River for the Moxos and Ciudad Bolívar on the lower Orinoco River for the Orinoco. The lines show functions that predict flooded area (Y, in km^2) from river stage (X, in m). For the Moxos at falling river stages, the predictive equation is $Y = 51{\cdot}109X + 193{\cdot}064X^2 + 9916$ ($r^2 = 0{\cdot}90$, $n = 48$). For the Moxos at rising river stages, the equation is $Y = 1296{\cdot}12X - 104{\cdot}044X^2 + 16{\cdot}423X^3 + 3139$($r^2 = 0{\cdot}90$, $n = 54$). For the Orinoco, the equation is $Y = -2388{\cdot}47X + 423{\cdot}344X^2 + 10\,784$ ($r^2 = 0{\cdot}90$, $n = 84$)

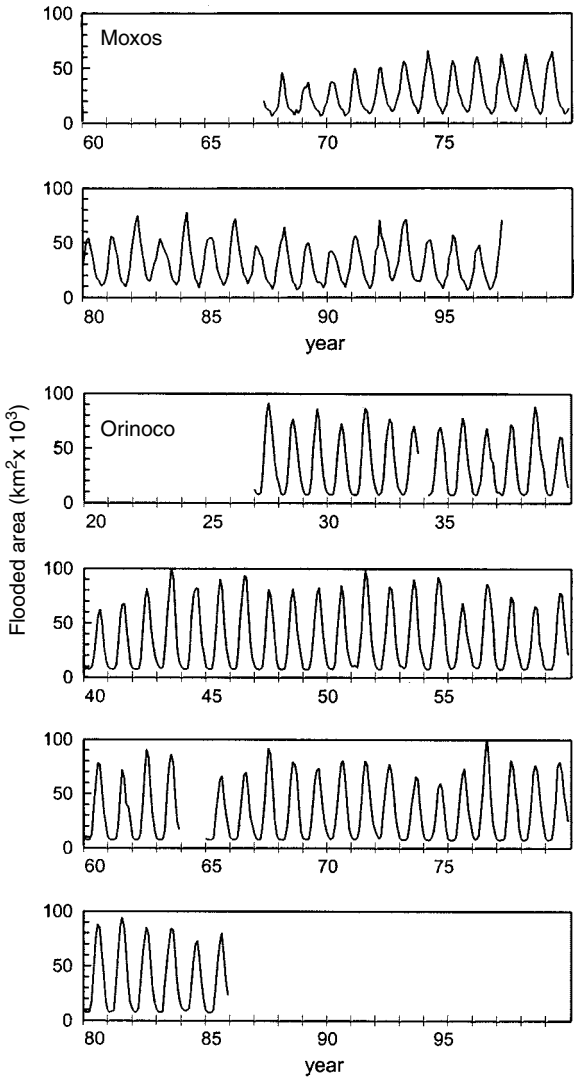

Figure 9. Extension of the inundation record using records of river stage and the predictive equations shown in Figure 8

whereas the timing and extent of inundation is much more variable among years. Floodplain inundation in the Llanos de Moxos tends to peak in March and April, a few months later than the months of maximum rainfall (December–February: Hanagarth 1993). Similarly, in the Llanos del Orinoco inundation peaks later (July–September) than the maximum rainfall (May–August: Machado-Allison, 1990). These time lags reflect the movement of river runoff from upland catchments to the floodplains as well as the delay in drainage of inundated areas back to the rivers.

Total flooded area showed a curvilinear relationship with river stage in both floodplain regions, and the regression equations describing these relationships allow prediction of flooded area from stage (Figure 8). For the Llanos de Moxos, the functional relationships were different for falling and rising river stages (as defined by the monthly mean stage on the prediction date compared with that of the previous month), so we developed separate equations for falling and rising water.

We used these predictive equations to extend the inundation record over the longer time period for which river stage observations are available (Figure 9). These extended records of inundation provide an indication of interannual variability. The Llanos de Moxos inundation record, which could be extended over only 30 years, shows significant variability in both the maximum and minimum flooded area. However, this variation is much smaller than the variation in flooding displayed by the Pantanal wetland over the same period, where there was little floodplain inundation during an extended drought from 1960 to 1973 (Hamilton *et al*., 1996, 2002). The Moxos record, which includes the period from 1967 to 1973, shows a lower extent of inundation in 1969 and 1970 but more normal flooding during the remainder of the period. The long-term mean inundation area for the Llanos de Moxos is 29 453 km^2 and the median is 24 681 km^2 (including the 4780 km^2 of open-water area). In the Llanos del Orinoco, the extended record shows more consistent flooding and drainage but substantial variation in the maximum extent of inundation, as we observed during the SMMR observation period. The long-term mean inundation area for the Llanos del Orinoco is 34 700 km^2 and the median is 25 297 km^2 (including the 2080 km^2 of open-water area).

In this study we have used passive microwave remote sensing to document inundation patterns in the Llanos de Moxos and the Llanos del Orinoco, providing an unprecedented view of the hydrology of these large savanna floodplains. These data improve our understanding of these important wetland ecosystems and will be useful in a wide variety of applications.

ACKNOWLEDGEMENTS

This research was based upon work supported by the U.S. National Aeronautics and Space Administration under grants NAGW-4352, NAGW-2652 and NAGW-2724, and by the National Science Foundation under grant DEB-9 701 714. Our knowledge of the Llanos de Moxos was enhanced through discussions with S. Beck, R. Langstroth and T. Killeen. We are grateful to T. Killeen for Landsat images, M.O. Smith for allowing us to study his AVHRR imagery, and to L. Hess for copies of the JERS mosaics. We also wish to acknowledge the Brazilian Agência Nacional de Energia Elétrica for the Madeira River stage data and the Venezuelan Ministerio del Ambiente y de los Recursos Naturales Renovables for the Orinoco River stage data. This is contribution 1140 of the W. K. Kellogg Biological Station.

REFERENCES

Bartlett KB, Harriss RC. 1993. Review and assessment of methane emissions from wetlands. *Chemosphere* **26**: 261–320.

Beck SG, Moraes M. 1997. Llanos de Mojos region (Bolivia). In *Centres of Plant Diversity: a Guide and Strategy for their Conservation*, *Vol. 3, The Americas*, Davis SD, Heywood VH, Herrera-MacBryde O, Villa-Lobos J, Hamilton AC (eds). World Wide Fund for Nature and the International Union for the Conservation of Nature: Cambridge, UK.

Campbell KE, Frailey CD, Arellano J. 1985. The geology of the Río Beni: further evidence for Holocene flooding in Amazonia. *Natural History Museum of Los Angeles County, Contributions in Science* **364**: 1–18.

Choudhury BJ. 1989. Monitoring global land surface using Nimbus-7 37 GHz data, theory and examples. *International Journal of Remote Sensing* **10**: 1579–1605.

Choudhury BJ. 1991. Passive microwave remote sensing contribution to hydrological variables. *Surveys in Geophysics* **12**: 63–84.

Denevan WM. 1966. *The aboriginal cultural geography of the Llanos de Mojos of Bolivia*. University of California Press: Berkeley.

Fu CC, Han D, Kim ST, Gloersen P. 1988. *User's guide for the Nimbus 7 Scanning Multichannel Microwave Radiometer (SMMR) CELL-ALL tape*. Reference Publication 1210, U.S. National Aeronautics and Space Administration: Washington, DC.

Gloersen P, Campbell WJ, Cavalieri DJ, Comiso JC, Parkinson CL, Zwally HJ. 1992. *Arctic and Antarctic Sea Ice, 1978–1987: Satellite Passive-Microwave Observations and Analysis*. NASA SP-511, National Aeronautics and Space Administration: Washington, DC.

Guyot JL, Wasson JG. 1994. Regional pattern of riverine dissolved organic carbon in the Amazon drainage basin of Bolivia. *Limnology and Oceanography* **39**: 452–458.

Haase R. 1992. Physical and chemical properties of savanna soils in northern Bolivia. *Catena* **19**: 119–134.

Haase R, Beck SG. 1989. Structure and composition of savanna vegetation in northern Bolivia: A preliminary report. *Brittonia* **41**: 80–100.

Hamilton SK. 1999. Potential effects of a major navigation project (the Paraguay-Paraná Hidrovía) on inundation in the Pantanal floodplains. *Regulated Rivers: Research and Management* **15**: 289–299.

Hamilton SK, Lewis WM Jr. 1990. Basin morphology in relation to chemical and ecological characteristics of lakes on the Orinoco River floodplain, Venezuela. *Archiv für Hydrobiologie* **119**: 393–425.

Hamilton SK, Sippel SJ, Melack JM. 1996. Inundation patterns in the Pantanal wetland of South America determined from passive microwave remote sensing. *Archiv für Hydrobiologie* **137**: 1–23.
Hamilton SK, Sippel SJ, Calheiros DF, Melack JM. 1997. An anoxic event and other biogeochemical effects of the Pantanal wetland on the Paraguay River. *Limnology and Oceanography* **42**: 257–272.
Hamilton SK, Sippel SJ, Melack JM. 2002. Comparison of inundation patterns in South American floodplains. *Journal of Geophysical Research* **107**(D20): DOI: 10.1029/2000JD000306.
Hanagarth W. 1993. *Acerca de la geoecología de las sabanas del Beni en el noreste de Bolivia*. Instituto de Ecología: La Paz, Bolivia. 186 pp.
Hastenrath S. 1990. Diagnostics and prediction of anomalous river discharge in northern South America. *Journal of Climate* **3**: 1080–1096.
Herrera JI, Rondón J. 1985. Estudio fotogeomorfológico del Río Orinoco y confluencia con el Río Apure. Sector Puerto Ayacucho, Río Caura. In *I Simposio Amazónico*, M.I. Muñoz (ed). *Boletín de Geología (Venezuela), Publicación Especial* **10**: 361–372.
Junk WJ. 1993. Wetlands of tropical South America. In *Wetlands of the World: Inventory, Ecology and Management*, Vol. I, Whigham DF, Dykyjová D, Hejný S (eds). Kluwer: Dordrecht; 679–739.
Junk WJ. 1997. *The Central Amazon Floodplain: Ecology of a Pulsing System*. Ecological Studies*, Vol. 126*, Springer: New York.
Junk WJ, Bayley PB, Sparks RE. 1989. The flood-pulse concept in river-floodplain systems. In *Proceedings of the International Large River Symposium*, Dodge DP (ed.). *Canadian Special Publication of Fisheries and Aquatic Sciences* **106**: 110–127.
Justice CO, Townshend JRG, Choudhury BJ. 1989. Comparison of AVHRR and SMMR data for monitoring vegetation phenology on a continental scale. *International Journal of Remote Sensing* **10**: 1607–1632.
Langstroth RP. 1996. *Forest islands in an Amazonian savanna of northeastern Bolivia*. Doctoral dissertation, Department of Geography, University of Wisconsin-Madison; 425 pp.
Lewis WM Jr, Saunders JF III. 1989. Concentration and transport of dissolved and suspended substances in the Orinoco River. *Biogeochemistry* **7**: 203–240.
Lewis WM Jr, Hamilton SK, Saunders JF III. 1995. Rivers of northern South America. In *Ecosystems of the world: Rivers*, Cushings C, Minshall GW, Cummins K (eds). Elsevier: Amsterdam; 219–256.
Lewis WM Jr, Hamilton SK, Lasi MA, Rodríguez M, Saunders JF III. 2000. Ecological determinism on the Orinoco floodplain. *BioScience* **50**: 681–692.
Machado-Allison A. 1990. Ecología de las áreas inundables de los Llanos de Venezuela. *Interciencia* **15**: 411–423.
Meade RH, Nordin CFJ, Pérez Hernández D, Mejia A, Pérez Godoy JM. 1983. Sediment and water discharge in Río Orinoco, Venezuela and Colombia. *Proceedings of the Second International Symposium on River Sedimentation*, 11–16 Oct 1980 Beijing, China.
Mertes LA, Dunne T, Martinelli LA. 1996. Channel-floodplain geomorphology along the Solimões-Amazon River, Brazil. *Geological Society of America Bulletin* **108**: 1089–1107.
Montes R, San José JJ. 1995. Vegetation and soil analysis of topo-sequences in the Orinoco Llanos. *Flora* **190**: 1–33.
Nordin C, Pérez Hernández D. 1989. *Sand Waves, Bars, and Wind-blown Sands of the Rio Orinoco, Venezuela and Colombia*. Water-supply Paper 2326-A, U.S. Geological Survey Reston, Virginia, USA.
Pérez Hernández D, Luís López J. 1998. Procesos geomorfológicos y estructuras sedimentarias en el Río Orinoco. In *El Río Orinoco: Aprovechamiento sustentable*, Luís López J, Ignacio Saavedra Cuadra I, Dubois Martínez M (eds). Universidad Central de Venezuela: Caracas; 138–154.
Plafker G. 1964. Oriented lakes and lineaments of northeastern Bolivia. *Geological Society of America Bulletin* **75**: 503–522.
Ramia M. 1967. Tipos de sabanas en los Llanos de Venezuela. *Boletín de la Sociedad Venezolana de Ciencias Naturales* **112**: 264–288.
Richey JE, Mertes LAK, Dunne T, Victoria RL, Forsberg BR, Tancredi C, Oliveira E. 1989. Sources and routing of the Amazon River flood wave. *Global Biogeochemical Cycles* **3**: 191–204.
San José JJ, Montes R. 1989. An assessment of regional productivity: the *Trachypogon* savannas at the Orinoco Llanos. *Nature and Resources* **25**: 5–18.
Sarmiento G. 1983. The savannas of tropical America. In *Tropical savannas*, Bourliere F (ed.). *Ecosystems of the World* **13**: 245–288.
Saunders JF III, Lewis WM Jr. 1988. Transport of phosphorus, nitrogen, and carbon by the Apure River, Venezuela. *Biogeochemistry* **5**: 323–342.
Sippel SJ, Hamilton SK, Melack JM, Choudhury BJ. 1994. Determination of inundation area in the Amazon River floodplain using the SMMR 37 GHz polarization difference. *Remote Sensing of Environment* **48**: 70–76.
Sippel SJ, Hamilton SK, Melack JM, Novo EMM. 1998. Passive microwave observations of inundation area and the area/stage relation in the Amazon River floodplain. *International Journal of Remote Sensing* **19**: 3055–3074.
Smith LK, Lewis WM Jr, Chanton JP, Cronin G, Hamilton SK. 2000. Methane emissions from the Orinoco River floodplain, Venezuela. *Biogeochemistry* **51**: 113–140.
Tamayo F. 1961. *Los Llanos de Venezuela.* Instituto Pedagógico, Dirección de Cultura: Caracas.
Welcomme RL. 1985. *River Fisheries*. FAO Fisheries Technical Paper 262, Food and Agriculture Organization: Rome; 330 pp.

